ORNL/TM-11490

ornl

OAK RIDGE NATIONAL LABORATORY

MARTIN MARIETTA

Resonance Analysis of the ^{239}Pu Neutron Cross Sections in the Energy Range 300 to 2000 eV

H. Derrien
G. de Saussure

OPERATED BY
MARTIN MARIETTA ENERGY SYSTEMS, INC.
FOR THE UNITED STATES
DEPARTMENT OF ENERGY

ORNL/TM-11490

Engineering Physics and Mathematics Division

RESONANCE ANALYSIS OF THE ^{239}Pu NEUTRON CROSS SECTIONS IN THE ENERGY RANGE 300 TO 2000 eV

H. Derrien and G. de Saussure

DATE PUBLISHED — June 1990

Prepared for the
Office of Energy Research
Division of Nuclear Physics

Prepared by the
OAK RIDGE NATIONAL LABORATORY
Oak Ridge, Tennessee 37831
operated by
MARTIN MARIETTA ENERGY SYSTEMS, INC.
for the
U.S. DEPARTMENT OF ENERGY
under contract DE-AC05-84OR21400

CONTENTS

ACKNOWLEDGMENTS vii
ABSTRACT ix
1. INTRODUCTION 1
2. EXPERIMENTAL DATA BASE AND METHOD OF ANALYSIS . . 2
3. RESULTS OF THE ANALYSIS 4
4. COMPARISON OF THE EVALUATION WITH MEASUREMENTS . . 7
5. CONCLUSION 17
REFERENCES 18

LIST OF FIGURES

Fig.		Page
1	Comparison of computed and measured ^{239}Pu cross sections between 450 and 500 eV	9
2	Comparison of computed and measured ^{239}Pu cross sections between 600 and 650 eV	10
3	Comparison of computed and measured ^{239}Pu cross sections	11
4	Comparison of computed and measured ^{239}Pu cross sections	12
5	Comparison of computed and measured ^{239}Pu cross sections	13
6	Comparison of computed and measured ^{239}Pu cross sections	14
7	Comparison of computed and measured ^{239}Pu cross sections	15
8	Comparison of computed and measured ^{239}Pu cross sections	16

LIST OF TABLES

Table		Page
1	2200 m/s values of cross sections	4
2	Comparison of average fission and capture widths and local strength functions	5
3	Average fission width of 1^+ levels and local strength functions	5
4	Comparison of average cross sections (b)	7
5	Comparison of average cross sections (b)	8

ACKNOWLEDGMENTS

The authors wish to acknowledge the considerable help of N. M. Larson and are indebted to L. W. Weston and J. A. Harvey for providing their data prior to publication and for helpful discussions about their measurements. The authors are also indebted to Sue Damewood for preparing this report.

ABSTRACT

A recent high-resolution measurement of the neutron fission cross section of ^{239}Pu has allowed the extension from 1 to 2 keV of a previously reported resonance analysis of the neutron cross sections, and an improvement of the previous analysis in the range 0.3 to 1 keV. Extensive tabular and graphical comparisons between results of measurements and calculations with the resonance parameters are given. The evaluation in ENDF-6 format is available at the nuclear data centers (NNDC at Brookhaven National Laboratory and NEADB at Saclay).

1. INTRODUCTION

The results of the ^{239}Pu fission cross-section measurement reported in 1984 by Weston and Todd[1] and recent transmission measurements of Harvey et al.[2] were analyzed up to 1 keV.[3] The 1984 fission cross-section measurement of Weston and Todd was done on a 20-m flight path and the instrumental resolution of the measurement was not sufficient to carry the resonance analysis beyond 1 keV. A new fission cross-section measurement on an 80-m flight path has recently been completed by Weston and Todd.[4] The resolution of this new measurement is comparable to that of the transmission measurements of Harvey et al. (also done on a 80-m flight path) and permits extension of the resonance analysis to higher energies. The purpose of this report is to describe the results of a consistent multilevel resonance analysis, from 300 eV to 2 keV, of the new fission cross-section measurement of Weston and Todd and of the transmission measurements of Harvey et al.

The results of the analysis in ENDF-6 are available at the nuclear data centers (NNDC at Brookhaven National Laboratory and NEADB at Saclay) and have been submitted for inclusion into JEF-2[5] and ENDF/B-VI.[6]

2. EXPERIMENTAL DATA BASE AND METHOD OF ANALYSIS

The resonance analysis computer code SAMMY[7] was utilised to perform the analysis, using the Reich-Moore multilevel R-matrix formalism.[8] In the energy region 300 to 1000 eV, a prior set of resonance parameters was available, obtained from the previous analysis.[3] The new fission cross-section measurement of Weston and Todd was added to the previously used data base. Because of the improvement in the resolution of the fission cross-section measurement, additional resonances had to be included and the process of analysis was repeated including the entire data base previously used. In the energy region 1 to 2 keV, no prior set of resonance parameters was available, and the initial input values to the SAMMY analysis were guessed from a graphical examination of the fission cross-section and transmission measurements.

All the resonances were taken as s-wave resonances. The p-wave penetration factor is approximately 0.005 at 1 keV; therefore, some of the small resonances in the 1 to 2 keV energy range could, in fact, be p-wave resonances, but existing data do not permit discrimination between the smaller s-wave and the large p-wave resonances. Spin assignments were made assuming that the resonances with a fission width larger than 300 meV were 0^+ resonances and that all others were 1^+. At the higher energies, some very wide resonances are hidden by the contributions of smaller resonances and can hardly be detected: 45 wide resonances were observed in the interval 1 to 1.5 keV, and 24 in the interval 1.5 to 2 keV, while below 1 keV, more than 50 wide resonances were observed in each 0.5-keV interval. Above 1 keV, no attempt was made to search for capture widths: a value of 46 meV was used for all the resonances. This value is the average value obtained for all the resonances in the interval 0.5 to 1 keV in the previous analysis.[3]

The final set of resonance parameters results from a somewhat incomplete analysis of the new fission cross-section measurement of Weston and Todd and of the thick sample (0.074 at/b) transmission measurement of Harvey et al. Lack of time has prevented the inclusion of the medium-thickness sample (0.018 at/b) transmission measurement of Harvey et al. into the analysis. Inclusion of that measurement would have improved the accuracy of the neutron widths of the larger resonances. Nevertheless, the resonance parameters obtained in the 1 to 2 keV region reproduce well the results of the fission cross section and transmission measurements and should provide a more accurate calculation of self-shielding factors than the alternative unresolved resonance formalism.

The previous resonance analysis up to 1 keV[3] indicated that the 1984 fission cross-section measurement of Weston and Todd was free of residual background. A consistent analysis of that fission measurement and of the transmission measurements of Harvey et al. did not require any renormalization or residual background adjustment. However, a consistent analysis of the transmission measurements and of the 1984 and 1988 fission cross-section measurements indicated the necessity of adding a smooth cross-section contribution to the resonance parameter contribution. The need for this smooth contribution is not fully understood. Above 1 keV, a smooth cross section, given in the ENDF/B File 3 Format, should be added to the fission cross section obtained from the resonance parameters given here in order to match the evaluated fission cross section.

3. RESULTS OF THE ANALYSIS

Two sets of resonance parameters were obtained: one describes the energy range up to 1 keV, the other describes the range 1 to 2 keV. The parameters describing the range up to 1 keV have been updated from the previous evaluation[3] in the thermal range and above 300 eV, based on the analysis of the new high resolution fission cross-section measurement of Weston and Todd.[6] The scattering radius has been reduced from 9.46 fm in the previous evaluation to 9.41 fm in the present evaluation as a consequence of a small renormalization of the transmission data of Harvey et al.[2] resulting from a reevaluation of the amount of aluminum in the ^{239}Pu samples used in the measurements. The values obtained for the 2200 m/s cross sections and for the Westcott g-factors with the new resonance parameters are compared to the values recommended by the ENDF/B-VI standards committee[9] in Table 1.

Table 1. 2200 m/s values of cross sections

Cross section	This work (b)	ENDF/B-VI Standards[9] (b)
Fission	747.08	747.99 ± 1.87
Capture	271.39	271.43 ± 2.14
Scattering	8.00	7.88 ± 0.97
Total	1027.47	1027.30
g_f	1.0555	1.0563 ± .0022
g_a	1.0794	1.0782 ± .0024

Above 300 eV, more resonances have been identified and the fission widths are more accurate than in the previous evaluation.[3] The average fission and capture widths and the local strength functions from the two evaluations are compared in Table 2. As can be seen from the table, the main effect of the inclusion of the new high-resolution fission cross-section measurement of Weston and Todd in the analysis has been to reduce the value of the fission widths, particularly in the ranges 600 to 700 and 800 to 900 eV. In these regions the accuracy of the fission widths has much improved.

In the energy range 1 to 2 keV, 364 resonances have been identified, versus 396 below 1 keV. Therefore, the number of missed resonances above 1 keV can be expected to be of the order of 10% and the values of the resonance parameters are probably not much distorted by unobserved or unresolved resonances.

As previously explained, some wide resonances were probably not detected at the higher energies. The contribution of these undetected resonances may explain part of the smooth contribution, increasing with energy, required in the analysis of the fission cross section. Additional wide resonances could be identified with further work.

Table 2. Comparison of average fission and capture widths and local strength functions

Energy range (keV)	Fission width (meV)		Capture width (meV)		Strength function ($\times 10^{-4}$)	
	1987	1989	1987	1989	1987	1989
0.3–0.4	23.4	22.1	44.6	46.1	0.912	0.922
0.4–0.5	52.5	49.2	41.0	44.9	0.723	0.731
0.5–0.6	31.2	32.2	48.1	46.6	1.992	1.991
0.6–0.7	25.4	17.4	43.7	43.4	0.807	0.814
0.7–0.8	25.5	24.4	46.3	46.4	0.786	0.800
0.8–0.9	75.3	50.2	45.6	47.1	0.794	0.805
0.9–1.0	68.4	64.2	45.1	41.4	1.290	1.343
0.3-1.0	43.1	37.1	44.4	45.1	1.043	1.058

As stated before, all the resonances observed were assumed to be excited by s-waves. The effect of possibly including some p-wave resonances in the calculation of the s-wave strength function is negligible compared to the effect of missing small s-wave resonances. The local strength functions, obtained by summing the reduced neutron widths $g\Gamma_n^0$, are listed in Table 3. The s-wave strength function over the interval 1 to 2 keV, $(0.935 \pm 0.090) \times 10^{-4}$ is smaller than the value, $(1.145 \pm 0.082) \times 10^{-4}$ obtained in the previous analysis[3] for the region up to 1 keV. This difference may be due to the missing contribution of unidentified wide resonances. The strength function obtained over the interval 0 to 2 keV is $(1.040 \pm 0.060) \times 10^{-4}$.

Table 3. Average fission width of 1^+ levels and local strength functions

Energy range (keV)	Fission width (meV)	Strength Function ($\times 10^{-4}$)
1.0-1.1	47.26	1.115
1.1-1.2	37.50	0.972
1.2-1.3	55.00	0.976
1.3-1.4	69.14	1.055
1.4-1.5	32.60	0.751
1.5-1.6	15.19	0.636
1.6-1.7	65.33	0.955
1.7-1.8	48.93	1.066
1.8-1.9	57.30	1.094
1.9-2.0	44.56	0.724
1.0-2.0	47.29	0.934

6 *RESULTS OF THE ANALYSIS*

The average fission widths in the interval 1 to 2 keV of the narrower resonances assumed to be 1^+ levels are listed in Table 3. On the average, these fission widths are larger than those of the range below 1 keV listed in Table 2. The fission widths above 1 keV may be overestimated because of the uncertainties due to the large value of the experimental resolution width, and because the narrower 0^+ levels could not been identified. Typical values of the instrumental and Doppler widths are 655 meV and 600 meV, respectively, at 1 keV. These values are large compared to the average total width of about 80 meV of the 1^+ resonances.

The average fission width in the interval 1.5 to 1.6 keV is particularly small, as is the case in the interval 0.55 to 0.65 keV. These minima in the average fission cross section may be evidence for a double humped 1^+ fission barrier.[10]

4. COMPARISON OF THE EVALUATION WITH MEASUREMENTS

The average cross sections calculated with the resonance parameters, in the interval 300 to 1000 eV, are compared with experimental data in Table 4. The 1976 absorption cross section and alpha measurements of Gwin et al.[11] were not used in the resonance parameter analysis, the average values obtained from these measurements agree to within a few percent with the values computed with the resonance parameters.

Table 4. Comparison of average cross sections (b)

Energy range (keV)	Fission		Capture	Absorption		Alpha	
	calc[a]	Ref 1	calc[a]	calc[a]	Ref 11	calc[a]	Ref 11
0.3–0.4	8.12	8.13	9.83	17.95	18.31	1.21	1.16
0.4–0.5	9.32	9.34	4.07	13.39	13.56	0.44	0.44
0.5–0.6	14.94	15.17	11.12	26.06	26.54	0.74	0.72
0.6–0.7	4.34	4.19	6.51	10.85	11.57	1.50	1.54
0.7–0.8	5.34	5.38	5.01	10.35	10.52	0.93	0.97
0.8–0.9	4.64	4.76	3.78	8.42	9.30	0.81	0.82
0.9–1.0	8.05	8.16	5.39	13.44	13.23	0.67	0.70
0.3–1.0	7.82	7.88	6.53	14.35	14.72	0.84	0.83

[a] Calculated from the resonance parameters.

The average fission and capture cross sections in the range 1 to 2 keV are compared to experimental data in Table 5. As previously explained, a smooth background has to be added to the resonance parameter contribution to obtain the evaluated fission cross section. The evaluated and experimental fission cross sections agree within 1 or 2 percent. The measured and computed capture cross sections averaged over the 1 to 2 keV range agree to better than 2%; however, over 100-eV intervals there are differences as large as 30%.

Figures 1 to 8 provide a detailed graphical comparison between the cross sections computed from the resonance parameters (solid lines) and the results of measurements. Comparison in the ranges 450 to 500 and 600 to 650 eV are shown in Figs. 1 and 2 respectively. The lowest curve in these figures shows the result of the 1984 fission cross section measurement of Weston and Todd, the curve just above shows the fission cross section from the 1988 measurement. The two upper curves in these figures show the effective total cross sections obtained from the thick and medium sample transmission measurements of Harvey et al. These figures illustrate the great improvement in instrumental resolution of the 1988 fission cross-section measurement of Weston and Todd over their 1984 measurement: almost all the resonances seen in the total cross-section measurement can also be seen in the 1988 fission cross-section measurement.

Table 5. Comparison of average cross sections (b)

Energy range	Fission			Capture	
(keV)	calc[a]	Ref 6	Eval[b]	calc[a]	Ref 19[c]
1.0–1.1	5.67	5.54	5.60	5.20	5.04
1.1–1.2	6.08	5.95	5.98	4.02	2.95
1.2–1.3	4.59	4.69	4.70	4.25	4.00
1.3–1.4	6.70	6.89	7.05	3.25	2.52
1.4–1.5	3.60	4.12	4.07	3.24	3.57
1.5–1.6	2.16	2.77	2.72	3.29	3.89
1.6–1.7	3.48	4.03	4.06	3.61	4.36
1.7–1.8	2.89	3.52	3.48	4.35	4.37
1.8–1.9	4.43	5.09	4.98	3.80	3.14
1.9–2.0	1.75	2.26	2.24	3.33	4.06
1.0–2.0	4.14	4.49	4.49	3.83	3.79

[a]Values calculated from the resonance parameters only.

[b]Values calculated from the resonance parameters and the smooth background file (File 3).

[c]The values of ref 19 have been renormalized to the values of ref 11.

Figures 3 to 8 show detailed comparisons in the range 1 to 2 keV. In these figures the lower curve represents the 1988 fission cross-section measurement of Weston and Todd, and the upper curve represents the effective total cross section obtained from the thick sample transmission measurement of Harvey et al. The vertical lines in the experimental data indicate the statistical standard deviations, the computed curves include the smooth contribution previously discussed.

An examination of the figures suggests that although the main features of the cross sections are well reproduced by the resonance parameters, considerable improvement in the fits to the measurements could be achieved with further work.

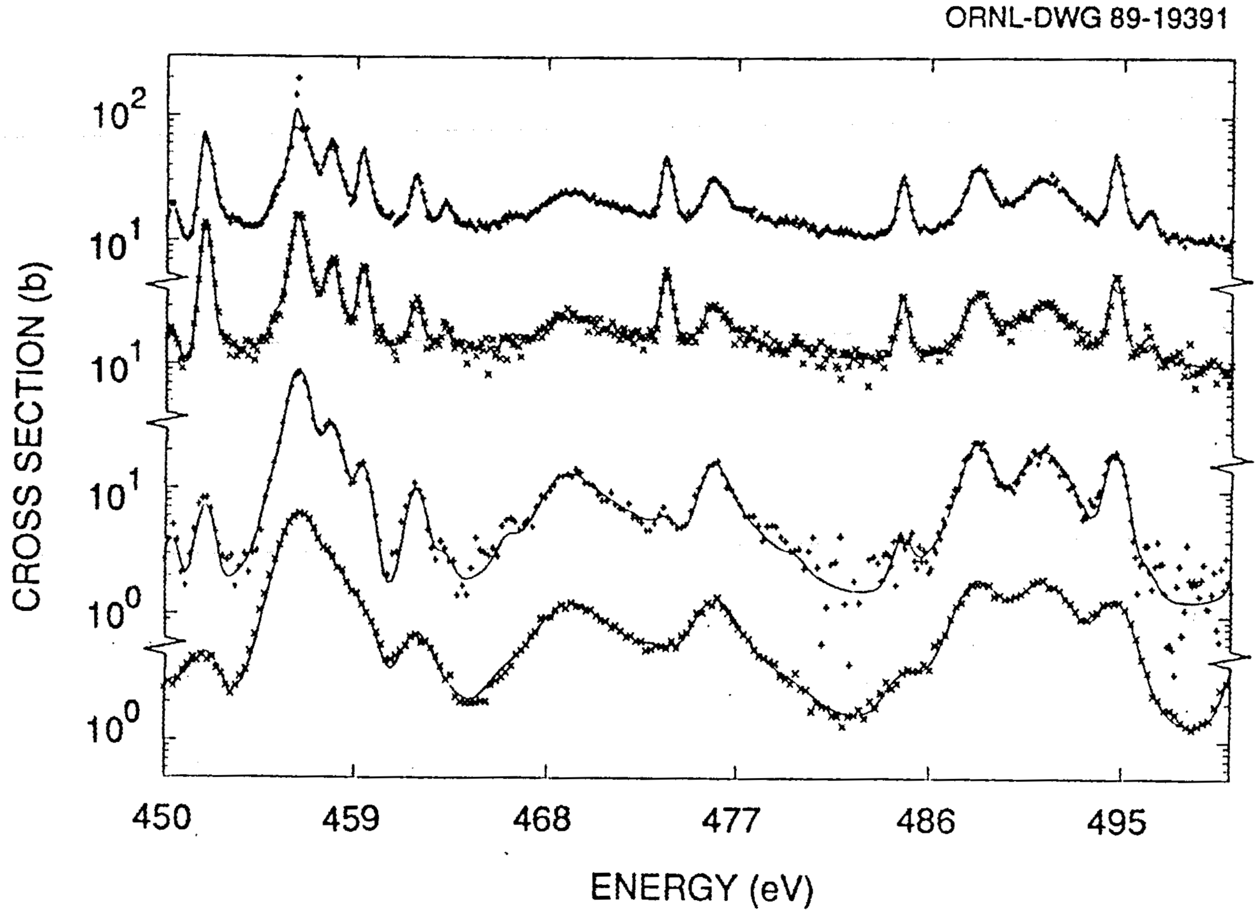

Fig. 1. Comparison of computed and measured ^{239}Pu cross sections between 450 and 500 eV. The solid lines were computed from the resonance parameters and broadened to correspond to the measurement conditions. The lower curve shows the result of the 1984 fission cross-section measurement of Weston and Todd. The curve just above shows the result of their 1988 measurement. The two upper curves show the effective total cross section as obtained from the thick sample (upper curve) and intermediate thickness sample transmission measurements of Harvey et al.

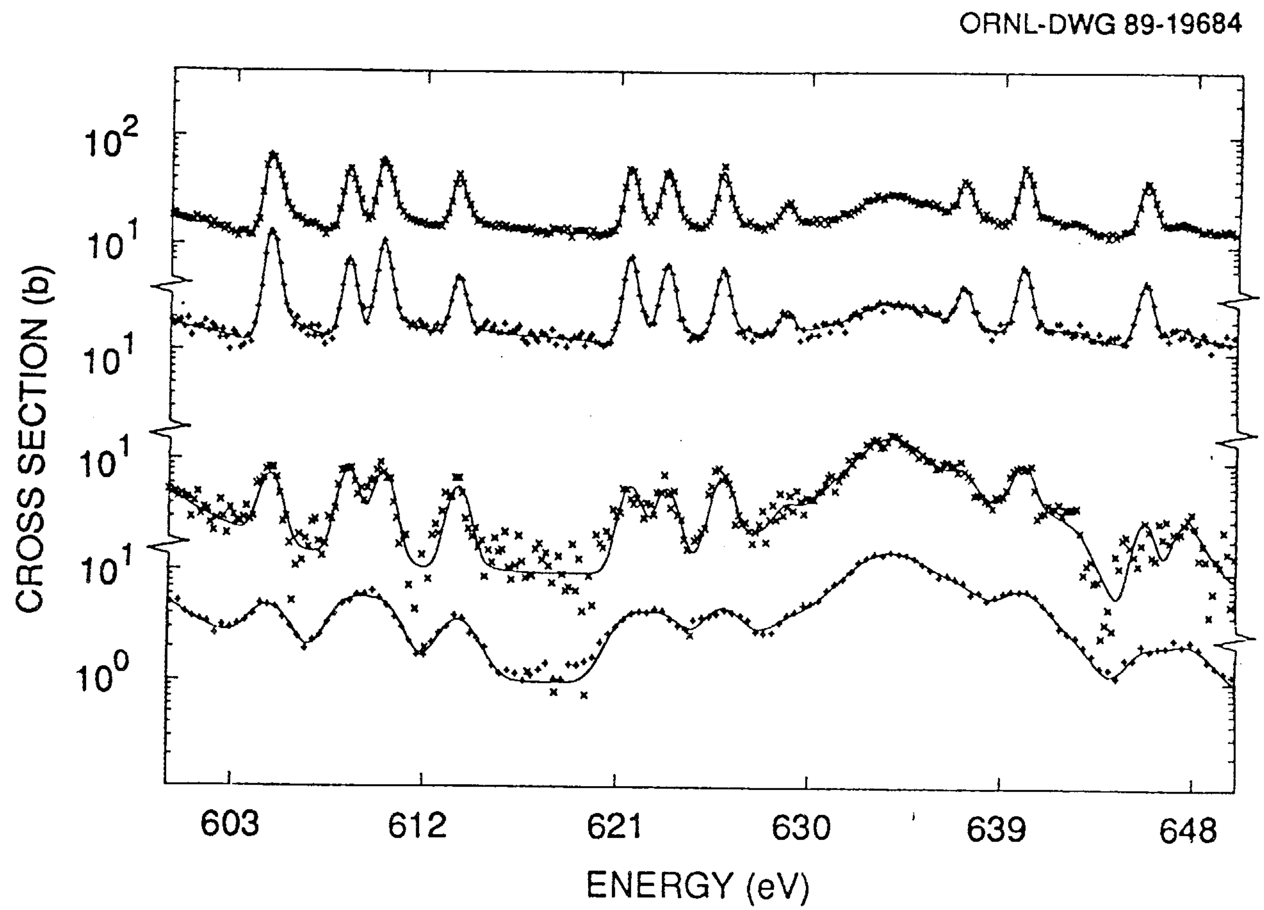

Fig. 2. Comparison of computed and measured ^{239}Pu cross sections between 600 and 650 eV. The solid lines were computed from the resonance parameters and broadened to correspond to the measurement conditions. The lower curve shows the result of the 1984 fission cross-section measurement of Weston and Todd. The curve just above shows the result of their 1988 measurement. The two upper curves show the effective total cross section as obtained from the thick sample (upper curve) and intermediate thickness sample transmission measurements of Harvey et al.

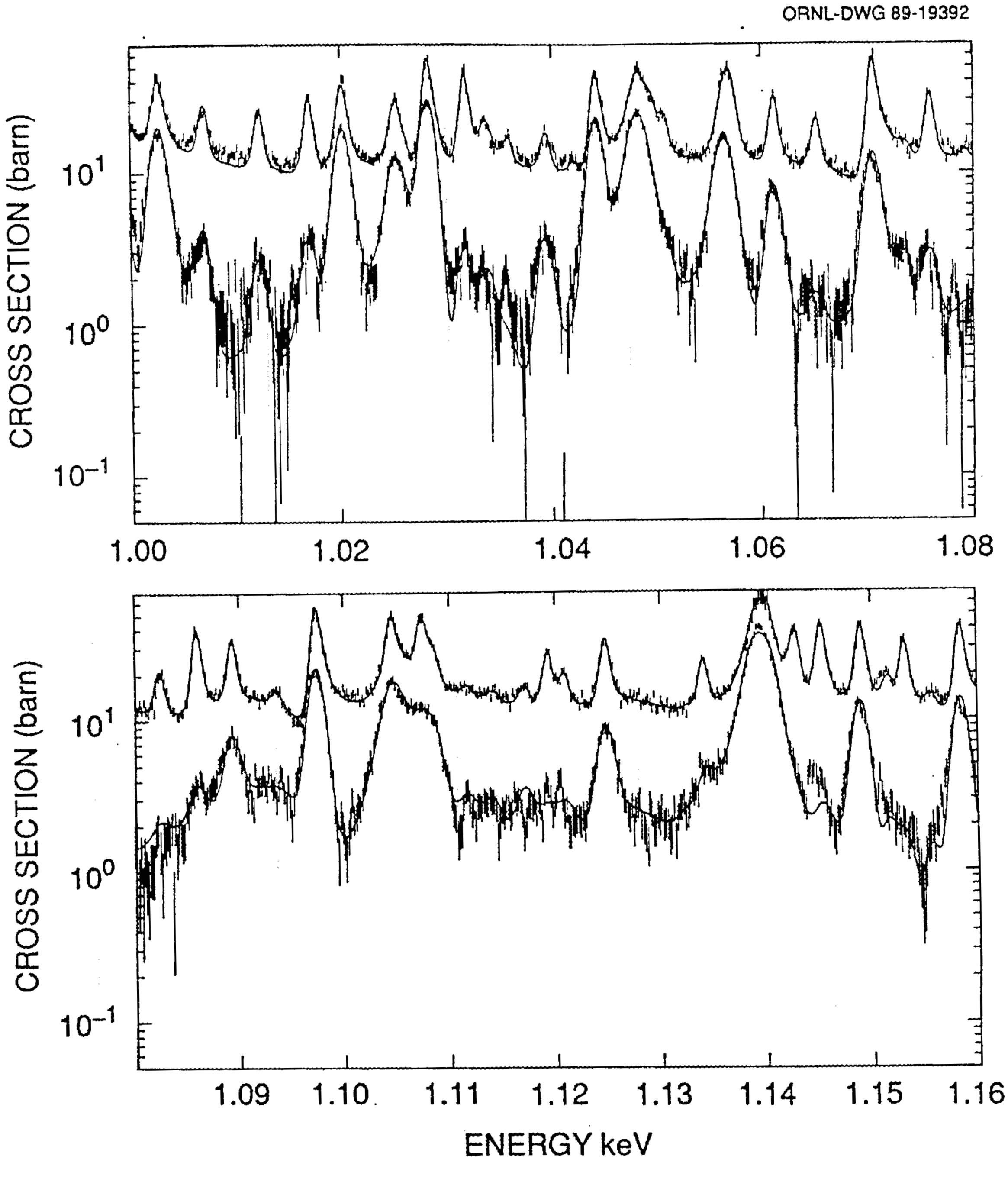

Fig. 3. Comparison of computed and measured ^{239}Pu cross sections. The neutron energy scale is indicated on the figure. The solid lines were computed from the resonance parameters including smooth contribution discussed in the text. The lower curve represent the result of the 1988 measurement of Weston and Todd. The upper curve shows the effective total cross section obtained from the thick sample transmission measurement of Harvey et al. The vertical lines of the data represent one statistical standard deviation.

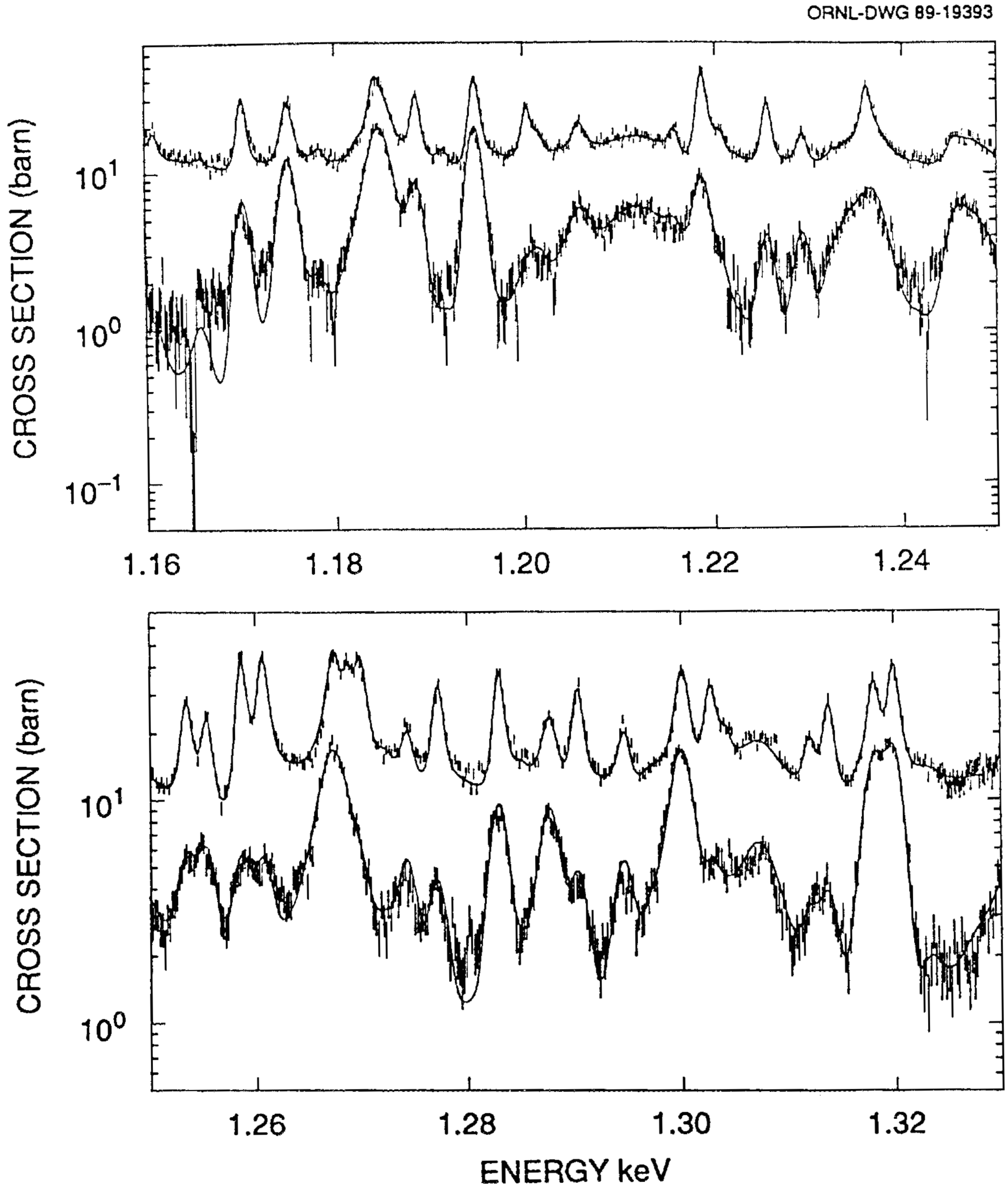

Fig. 4. Comparison of computed and measured ^{239}Pu cross sections. The neutron energy scale is indicated on the figure. The solid lines were computed from the resonance parameters including smooth contribution discussed in the text. The lower curve represent the result of the 1988 measurement of Weston and Todd. The upper curve shows the effective total cross section obtained from the thick sample transmission measurement of Harvey et al. The vertical lines of the data represent one statistical standard deviation.

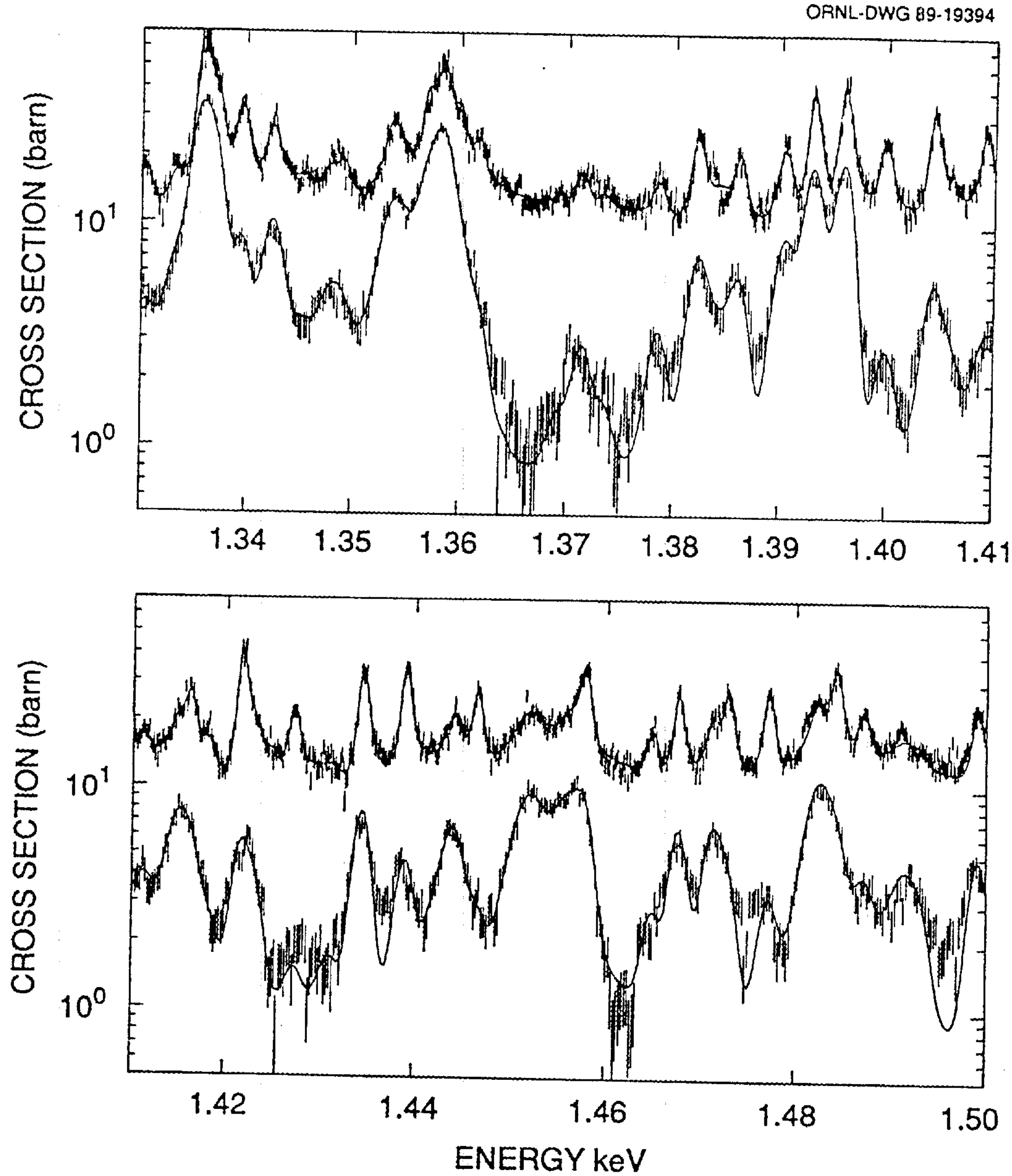

Fig. 5. Comparison of computed and measured ^{239}Pu cross sections. The neutron energy scale is indicated on the figure. The solid lines were computed from the resonance parameters including smooth contribution discussed in the text. The lower curve represent the result of the 1988 measurement of Weston and Todd. The upper curve shows the effective total cross section obtained from the thick sample transmission measurement of Harvey et al. The vertical lines of the data represent one statistical standard deviation.

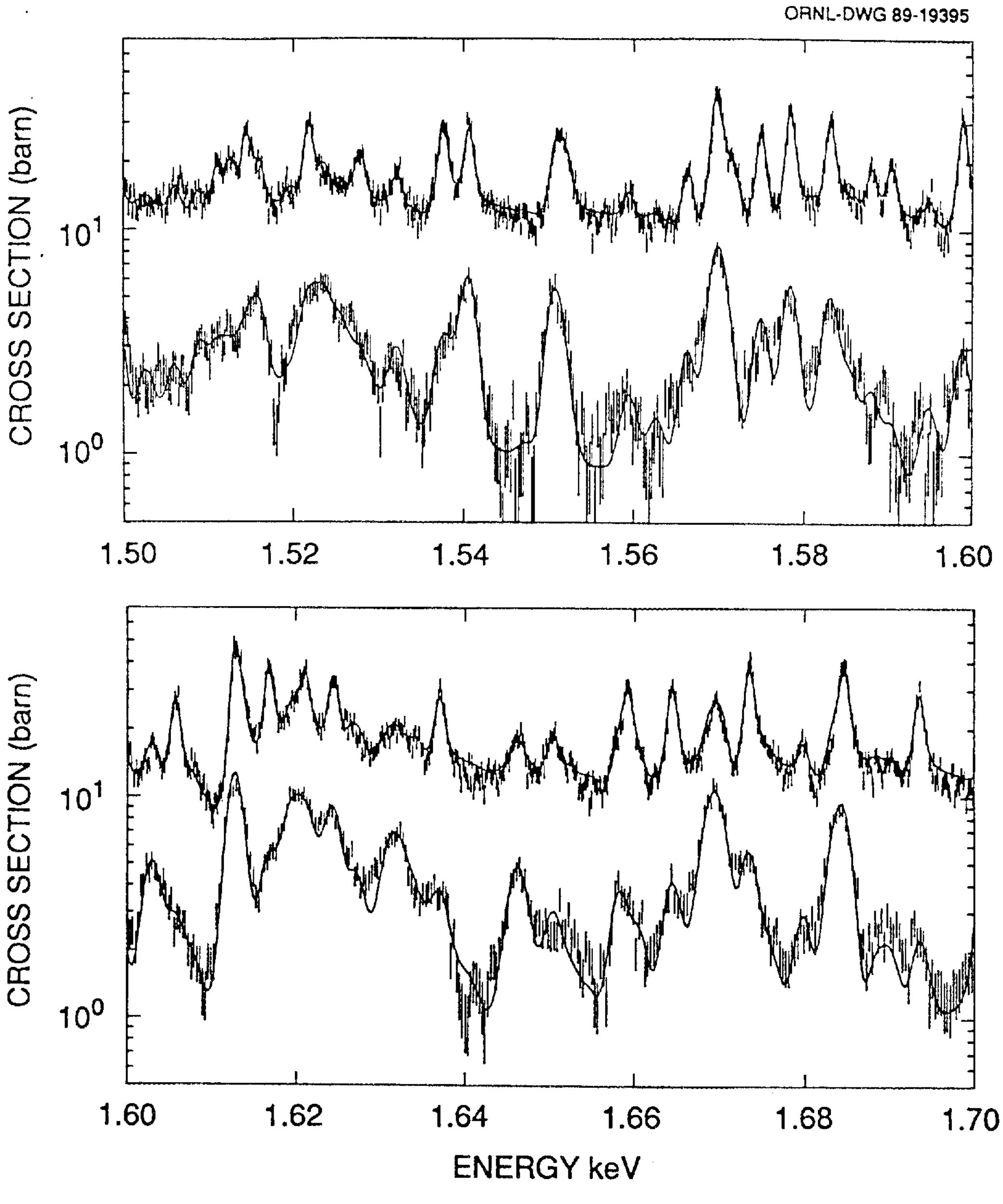

Fig. 6. Comparison of computed and measured ^{239}Pu cross sections. The neutron energy scale is indicated on the figure. The solid lines were computed from the resonance parameters including smooth contribution discussed in the text. The lower curve represent the result of the 1988 measurement of Weston and Todd. The upper curve shows the effective total cross section obtained from the thick sample transmission measurement of Harvey et al. The vertical lines of the data represent one statistical standard deviation.

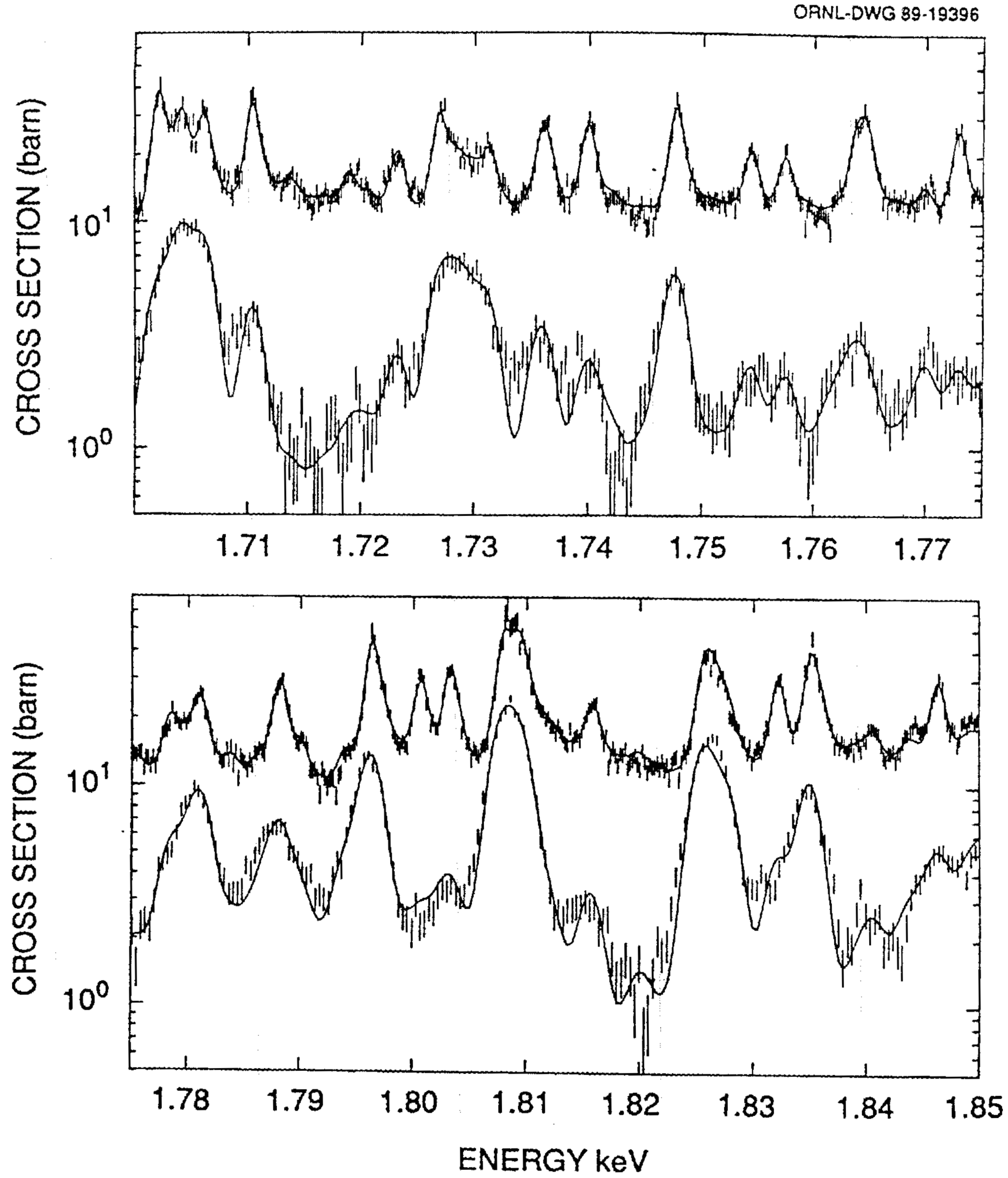

Fig. 7. Comparison of computed and measured ^{239}Pu cross sections. The neutron energy scale is indicated on the figure. The solid lines were computed from the resonance parameters including smooth contribution discussed in the text. The lower curve represent the result of the 1988 measurement of Weston and Todd. The upper curve shows the effective total cross section obtained from the thick sample transmission measurement of Harvey et al. The vertical lines of the data represent one statistical standard deviation.

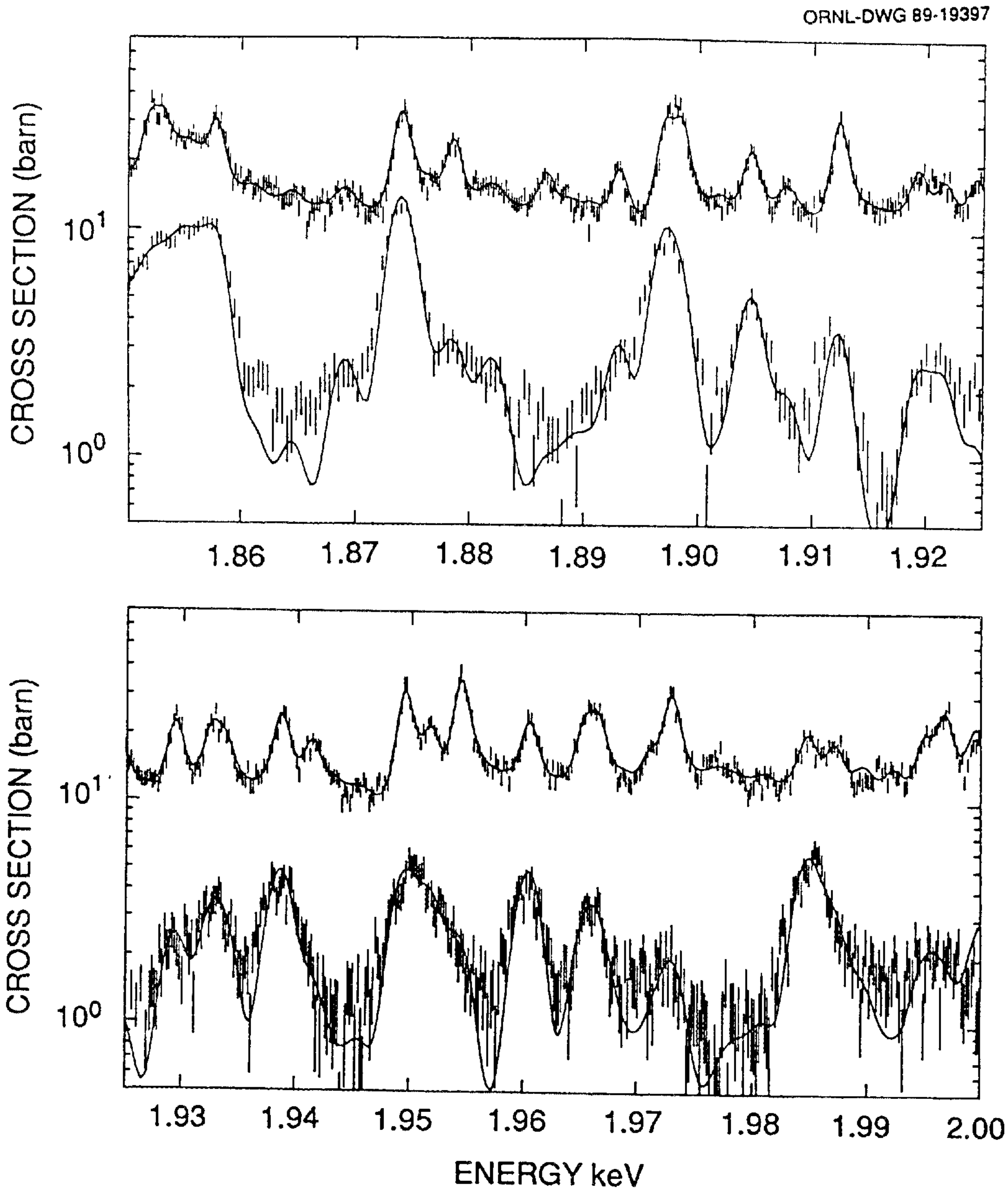

Fig. 8. Comparison of computed and measured ^{239}Pu cross sections. The neutron energy scale is indicated on the figure. The solid lines were computed from the resonance parameters including smooth contribution discussed in the text. The lower curve represent the result of the 1988 measurement of Weston and Todd. The upper curve shows the effective total cross section obtained from the thick sample transmission measurement of Harvey et al. The vertical lines of the data represent one statistical standard deviation.

5. CONCLUSION

The good instrumental resolution of the 1988 fission cross-section measurement of Weston and Todd has allowed the extension of the resonance analysis of the ^{239}Pu neutron cross sections from 1 to 2 keV and a significant improvement of the analysis in the region 0.3 to 1 keV. Lack of time has prevented us from carrying the analysis as far as would have been desirable. In particular, the inclusion of the results of the medium thickness transmission measurement of Harvey et al. in the resonance analysis above 1 keV would have yielded more accurate values of the neutron widths of the large resonances; a more systematic search for hidden wide resonances at the upper energy end of the analysis might have helped clarify some apparent inconsistencies between the fission cross section and transmission measurements and might have eliminated the need to introduce a smooth background component in the evaluation; a more thorough search for the resonance parameters would have improved the agreement between the calculated and measured cross sections above 1 keV. An extensive use of the Dyson-Metha Δ_3 statistic[12] to assign the spin of the resonances and to determine where small resonances should be added to help the fit might have improved the quality of the analysis. Indeed several authors have observed that the Δ_3 statistic is very sensitive to missing levels;[13,14] this statistic has proven very helpful in a similar analysis of the ^{235}U neutron cross sections.[15]

In spite of the shortcoming just discussed, we feel that the present analysis is a significant improvement over the previous one[3] in the energy region below 1 keV, and that in the range 1 to 2 keV the resonance parameters obtained provide a better estimate of resonance self-shielding than the unresolved resonance formalism. Indeed several recent studies have demonstrated that the use of the unresolved resonance formalism can lead to significant errors in the calculation of resonance selfshielding;[16,17,18] this is particularly true in the keV resonance range where self-shielding is most important.

REFERENCES

1. L. W. Weston and J. H. Todd, *Nucl. Sci. Eng.* **88**, 567 (1984).
2. J. A. Harvey et al., "High-Resolution Neutron Transmission Measurements on ^{235}U, ^{238}U, and ^{239}Pu," *Proc. Internat. Conf. Nuclear Data for Science and Technology*, Mito, Japan, May 30–June 3, p. 115 (1988).
3. H. Derrien and G. de Saussure, "Current Plutonium Cross Section Evaluations in the Resolved Resonance Region," *Proc. Internat. Reactor Physics Conf.* Jackson Hole, WY, Sept 18–22, papers S65 (1988); see also H. Derrien, G. de Saussure and R. B. Perez, "R-matrix Analysis of ^{239}Pu Neutron Cross Sections in the Energy Range up to 1000 eV," accepted for publication in Nucl. Sci. Eng. (1990).
4. L. W. Weston and J. H. Todd, "50 Years with Nuclear Fission," p. 957 (1989).
5. Joint Evaluated File, Nuclear Data Library, available from the Nuclear Data Centers.
6. Evaluated Nuclear Data File, available from the Nuclear Data Centers.
7. N. M. Larson, *Updated User's Guide for SAMMY: Multilevel R Matrix Fits of Neutron Data Using Bayes Equations*, ORNL/TM-9719/R2, Oak Ridge National Laboratory (1989); see also N. M. Larson and F. G. Perey, "Resonance Parameters Analysis with SAMMY," Proc. Internat. Conf. Nuclear Data for Science and Technology, Mito, Japan, May 30–June 3, p. 573 (1988).
8. C. W. Reich and M. S. Moore, *Phys. Rev.* **111**, 929 (1958).
9. A. Carlson et al., National Bureau of Standards, "Results of the ENDF/B-VI Standards Evaluation," Private Communication to C. Dunsford (Aug. 31, 1987).
10. J. Blons, H. Derrien and A. Michaudon, "Mesure a Haute Resolution et Analyse de la Section Efficace de Fission du Plutonium-239," Vol.II, p 513, Proceedings Second Internat. Conf. Nuclear Data for Reactors, Helsinki, 15–19 June (1977).
11. R. Gwin et al., *Nucl. Sci. Eng.* **59**, 79 (1976).
12. F. G. Dyson and M. L. Metha, *J. Math. Phys.* **4**, 701 (1963).
13. G. Carraro and Brusegan, *Nucl. Phys.* **A257**, 333 (1976).
14. H. I. Liou et al., *Phys. Rev.* **C5**, 974 (1972).
15. L. C. Leal et al., *Transactions Amer. Nucl. Soc.* **59**, 341 (1989).
16. J. L. Munoz-Cobos et al., *Nucl. Sci. Eng.* **81**, 55 (1982).
17. P. Ribon, V. Sauvinet and P. Moussalem, *Etude des Methodes de Calcul de l'Autoprotection dans les Resonances*, NEACRP-A-696, Comissariat a l'Energie Atomique, France (1985).
18. L. C. Leal et al., "Test of the ENDF/B unresolved resonance formalism for ^{235}U," *Transactions Amer. Nucl. Soc.* **60**, 620 (1989).
19. R. Gwin et al., *Nucl. Sci. Eng.* **45**, 25 (1971).

INTERNAL DISTRIBUTION

1. B. R. Appleton
2–6. G. de Saussure
7. J. K. Dickens
8. F. Difilippo
9. C. Y. Fu
10. J. A. Harvey
11. D. M. Hetrick
12. N. W. Hill
13. D. C. Larson
14. N. M. Larson
15. R. L. Macklin
16. F. C. Maienschein
17. R. W. Peelle
18. C. M. Perey
19. F. G. Perey
20. R. B. Perez
21. R. R. Spencer
22. L. W. Weston
23. R. Q. Wright
24. J. J. Dorning (consultant)
25. R. M. Haralick (consultant)
26. J. E. Leiss (consultant)
27. N. Moray (consultant)
28. M. F. Wheeler (consultant)
29. EPMD Reports Office
30–31. Laboratory Records Department
32. Laboratory Records, ORNL–RC
33. Document Reference Section
34. Central Research Library
35. ORNL Patent Section

EXTERNAL DISTRIBUTION

36. Office of the Assistant Manager for Energy Research and Development, Oak Ridge Operations, U.S. Department of Energy, Oak Ridge, TN 37831
37. E. D. Arthur, Los Alamos National Laboratory, P. O. Box 1663, MS-243, Group T-2, Los Alamos, NM 87545
38. G. F. Auchampaugh, Los Alamos National Laboratory, MS 442, P-3, Los Alamos, NM 87545
39. M. R. Bhat, Building 197D, National Nuclear Data Center, Brookhaven National Laboratory, Upton, NY 11973
40. R. C. Block, Department of Nuclear Engineering, Rensselaer Polytechnic Institute, Troy, NY 12180
41. A. D. Carlson, RADP B109, National Institute of Standards and Technology, Gaithersburg, MD 20899
42. C. Coceva, ENEA Comitato Nazionale, Centro Richerche Energie, Ezio Clemental, via G. Maxxini, 2, 40138, Bologna, Italy
43. H. Derrien, Route de Kerdaniou, 29133 La Foret Fouesnant, Finistere, France
44. E. Fort, Commissariat a l'Energie Atomique, Centre d'Etudes Nucleaires de Cadarache, Boite Postale No. 1, 13115 Saint-Paul-Lez-Durance, France
45. F. H. Fröehner, Institut für Neutronenphysik und Reaktortechnik, Kernforschungszentrum Karlsruhe, Postfach 3640, D-75 Karlsruhe, Federal Republic of Germany
46. R. N. Hwang, Argonne National Laboratory, Applied Physics Division, Argonne, IL 60439
47. Philip B. Hemmig, Chief, NE-542/GTN, Advanced Reactor Technology, U.S. Department of Energy, Washington, DC 20585
48. E. C. Lynn, Nuclear Physics Division, Atomic Energy Research Establishment, Harwell, Didcot, Oxon, OX11, ORA, United Kingdom

49. R. E. MacFarlane, Los Alamos National Laboratory, P. O. Box 1663 MS B342, Los Alamos, NM 87545
50. D. G. Madland, Los Alamos National Laboratory, P. O. Box 1663, Group T-2, MS B-243, Los Alamos, NM 87545
51. M. S. Moore, Los Alamos National Laboratory, P. O. Box 1663, MS 442, Los Alamos, NM 87545
52. G. L. Morgan, Los Alamos National Laboratory, P. O. Box 1663, Group P-15, MS D406, Los Alamos, NM 87545
53. T. Nakagawa, Japan Atomic Energy Research Institute, Tokai Research Establishment Linac Laboratory, Tokai-Mura, Naka-Gun, Ibaraki-Ken, Japan
54. S. Pearlstein, Brookhaven National Laboratory, Building 197D, National Nuclear Data Center, Upton, NY 11973
55. W. P. Poenitz, Argonne National Laboratory-West, P. O. Box 2528, Idaho Falls, ID 83403
56. M. Salvatores, Commissariat a l'Energie Atomique, Centre d'Edutes Nucleaires de Cadarache, Boite Postale No. 1, 13115 Saint-Paul-Lez-Durance, France
57. Donald L. Smith, Building 314, Engineering Physics Division, Argonne National Laboratory, 9700 South Cass Ave., Argonne, IL 60439
58. M. G. Sowerby, Nuclear Physics Division, Building 418, Atomic Energy Research Establishment, Harwell, Didcot, Oxon, OX11, ORA, United Kingdom
59. C. Wagemans, Central Bureau for Nuclear Measurements, Steenweg naar Retie, B-2400, Geel, Belgium
60. O. A. Wasson, Neutron Measurements & Research, National Institute of Standards and Technology, Gaithersburg, MD 20899
61. Herman Weigmann, Central Bureau for Nuclear Measurements, Steenweg naar Retie, B-2400, Geel, Belgium
62. S. L. Whetstone, Division of Nuclear Physics, ER 23/GTN, U.S. Department of Energy, Washington, DC 20585
63. R. M. White, Physics Department, MS L-298, Lawrence Livermore National Laboratory, P. O. Box 808, Livermore, CA 94550
64. R. R. Winters, Department of Physics, Denison University, Granville, OH 43023
65. P. G. Young, Los Alamos National Laboratory, MS-243, Group T-2, Los Alamos, NM 87545

66–75. Office of Scientific and Technical Information, P. O. Box 62, Oak Ridge, TN 37830